ORIGINAL ARTICLES

Evaluation of tolerance to lentiviral LV-RPE65 gene therapy vector after subretinal delivery in non-human primates

ALEXANDRE MATET, CORINNE KOSTIC, ALEXIS-PIERRE BEMELMANS, ALEXANDRE MOULIN, SERGE G. ROSOLEN, SAMIA MARTIN, FULVIO MAVILIO, VAZRIK AMIRJANIANS, KNUT STIEGER, BIRGIT LORENZ, FRANCINE BEHAR-COHEN, and YVAN ARSENIJEVIC

LAUSANNE, SWITZERLAND; FONTENAY-AUX-ROSES, ASNIÈRES, PARIS, EVRY, FRANCE; AND GIESSEN, GERMANY

Several approaches have been developed for gene therapy in RPE65-related Leber congenital amaurosis. To date, strategies that have reached the clinical stages rely on adeno-associated viral vectors and two of them documented limited long-term effect. We have developed a lentiviral-based strategy of RPE65 gene transfer that efficiently restored protein expression and cone function in RPE65-deficient mice. In this study, we evaluated the ocular and systemic tolerances of this lentiviral-based therapy (LV-RPE65) on healthy nonhuman primates (NHPs), without adjuvant systemic anti-inflammatory prophylaxis. For the first time, we describe the early kinetics of retinal detachment at 2, 4, and 7 days after subretinal injection using multimodal imaging in 5 NHPs. We revealed prolonged reattachment times in LV-RPE65–injected eyes compared to vehicle-injected eyes. Low- (n = 2) and high-dose (n = 2) LV-RPE65–injected eyes presented a reduction of the outer nuclear and photoreceptor outer segment layer thickness in the macula, that was more pronounced than in vehicle-injected eyes (n = 4). All LV-RPE65–injected eyes showed an initial perivascular reaction that resolved spontaneously within 14 days. Despite foveal structural changes, full-field electroretinography indicated that the overall retinal function was preserved over time and immunohistochemistry identified no difference in glial, microglial, or leucocyte ocular activation between

From the Unit of Retinal Degeneration and Regeneration, Department of Ophthalmology, University of Lausanne, Jules-Gonin Eye Hospital, Fondation Asile des Aveugles, Lausanne, Switzerland; Commissariat à l'Energie Atomique et aux Energies Alternatives (CEA), Direction de la Recherche Fondamentale (DRF), Institut d'Imagerie Biomédicale (I2BM), Molecular Imaging Research Center (MIRCen), Fontenay-aux-Roses, France; Centre National de la Recherche Scientifique (CNRS), Université Paris-Sud, Université Paris-Saclay, UMR 9199, Neurodegenerative Diseases Laboratory, Fontenay-aux-Roses, France; Pathology Unit, Department of Ophthalmology, University of Lausanne, Jules-Gonin Eye Hospital, Fondation Asile des Aveugles, Lausanne, Switzerland; Clinique Vétérinaire Voltaire, Asnières, France; UPMC Univ Paris 06, UMR_S 968, Centre de Recherche Institut de la Vision, Paris, France; Genethon, Evry, France; Department of Ophthalmology, Justus-Liebig-University Giessen, Giessen, Germany; Inserm U1138, Team 17, From Physiopathology of Ocular Diseases to Clinical Development, Université Paris Descartes Sorbonne Paris Cité, Centre de Recherche des Cordeliers, Paris, France.

Submitted for publication January 19, 2017; revision submitted April 30, 2017; accepted for publication June 30, 2017.

Reprint requests: Yvan Arsenijevic, Unit of Retinal Degeneration and Regeneration, Hôpital Ophtalmique Jules-Gonin, University of Lausanne, Avenue de France 15, Case Postale 5143, 1002 Lausanne, Switzerland; e-mail: yvan.arsenijevic@fa2.ch or Corinne Kostic, Group of Retinal Disorder Research, Hôpital Ophtalmique Jules-Gonin, University of Lausanne, Avenue de France 15, Case Postale 5143, 1002 Lausanne, Switzerland; e-mail: corinne.kostic@fa2.ch.

1931-5244/$ - see front matter

http://dx.doi.org/10.1016/j.trsl.2017.06.012

low-dose, high-dose, and vehicle-injected eyes. Moreover, LV-RPE65–injected animals did not show signs of vector shedding or extraocular targeting, confirming the safe ocular restriction of the vector. Our results evidence a limited ocular tolerance to LV-RPE65 after subretinal injection without adjuvant anti-inflammatory prophylaxis, with complications linked to this route of administration necessitating to block this transient inflammatory event. (Translational Research 2017;188:40–57)

Abbreviations: NHP = nonhuman primates; LE = left eye; RE = right eye; IOP = intraocular pressure; EZ = ellipsoid zone; ONL = outer nuclear layer; ERG = electroretinogram

AT A GLANCE COMMENTARY

Matet A, et al.

Background

Leber congenital amaurosis, a severe and early-onset form of retinitis pigmentosa is historically the first eye disease to benefit from gene therapy, with several groups worldwide developing AAV-based gene replacement approaches for *RPE65*, one of the causative genes. However, some clinical trials showed limited safety and only partial recovery which could be linked to the subretinal surgical route, or to subtherapeutic protein levels. Simultaneously, our group has developed a HIV-1–derived lentivirus-based strategy (LV-RPE65), using the high transduction capability of this vector to target epithelia such as the retinal pigment epithelium, which expresses the RPE65 enzyme. LV-RPE65 can restore photoreceptor integrity and function, as previously demonstrated by our group in 2 rodent models of RPE65 deficiency. In this study, we have pursued the translational development of LV-RPE65, to evaluate the ocular and systemic tolerance to LV-RPE65 after subretinal injection in 5 nonhuman primates without antiinflammatory prophylaxis.

Translational Significance

In the present study, the absence of systemic LV-RPE65 vector particle shedding after subretinal injection in body fluids, or of vector genome integration in various organs is promising for the ocular use of lentiviral vector. Nevertheless, a transient perivascular retinal reaction occurred at very early stages (2 days) following vector administration, and a thinning of the photoreceptor layer at the macula level was observed in all groups, including vehicle-treated animals. No other major ocular adverse event was recorded, except in one eye that inadvertently received intraocular doses due to a leak into the vitreous cavity. Importantly, we were not able to find any other preclinical study in the literature reporting ocular and retinal monitoring at early time points after subretinal gene therapy administration. Our report is thus the first to give insight into these early events and may contribute to elucidate several limitations of the subretinal route approach. These observations contribute to optimizing the translational process of retinal gene therapy, from both the surgical and the gene transfer perspectives, and highlight the necessity to improve lentiviral vector tolerance by antiinflammatory pretreatment.

INTRODUCTION

Retinal dystrophies, especially those with childhood onset, are a lifetime burden for affected individuals, with no available treatments. Recently, retinal gene therapy based on subtypes of adeno-associated virus (AAV)[1-6] or lentivirus-derived vectors[7-10] has made tremendous advances to correct several monogenic diseases in rodent and large animal models providing the ground to design first clinical trials and translate this technology in humans.[11] The first gene augmentation strategy in an inherited retinal disorder was developed clinically for patients with Leber congenital amaurosis due to RPE65 deficiency.[12] RPE65 is a retinal pigment epithelium (RPE)–expressed enzyme with isomerase activity, which plays a key role in the visual cycle by recycling chromophores necessary for the phototransduction.[13-15] Three main clinical trials initiated in the US[16,17] and UK[18] based on the AAV2/2-vector approach demonstrated a limited safety with partial, and in 2 trials transitory, visual function restoration. In one trial, inflammation induced by AAV2/2 vector at the highest dose required redesigning of the vector using an AAV5 capsid.[19] In addition, ongoing trials are conducted in Israel with the AAV2/2 vector developed by the group of Hauswirth,[20] and in France with the AAV2/4 vector.[21] The major visual improvements were attested using

dark-adapted perimetry,[22,23] that identified an increased retinal sensitivity in the treated area of certain patients. Functional magnetic resonance imaging of the visual cortex showed contrast discrimination enhancement, for a subset of patients[24] and mobility testing demonstrated the ability to better navigate after treatment in certain patients.[22,25] Differences in the effect of gene therapy between these different trials, or between treated patients, results probably from multiple factors, including the timing of intervention during disease course, surgical delivery techniques (administered volume, flow rate, procedure), vector designs, and patient genetic backgrounds. Moreover, subjective parameters used to reveal the effect of gene therapy such as visual acuity or retinal sensitivity testing might be biased, despite efficient viral transduction, because of cortical amblyopia following long-standing visual loss in early childhood.

The major hurdle experienced in these trials was that subretinal injection under the macula induced, in several patients, retinal thinning and/or foveal morphologic changes, which were not foreseeable and may have contributed to the lack of central vision restoration.[22,26] Because inclusion of control subjects receiving the buffer solution subretinally was not planned in these studies for obvious ethical reasons, it is not clear whether the surgery by itself is deleterious or whether the vector contributes to these unexpected retinal alterations.

In addition, despite improvements in visual sensitivity, the degenerative rate of the treated eye remained similar to the nontreated eye,[22,23] indicating either an unstoppable disease progression, inappropriate treatment delivery (timing of treatment, surgical techniques), or an insufficient vector efficacy.[19] The available amount of chromophore is determinant for photoreceptor function and survival, and consequently RPE65 expression levels are correlated to retinal function and to the rate of retinal degeneration in animal models. For instance, in the *Rpe65*$^{R91W/R91W}$ mouse model, where the amount of RPE65 is decreased by around 90%, electroretinography showed a 3-log reduction in retinal sensitivity at 1-month of age, as compared with wild-type mice, which is correlated to the level of RPE65 protein.[27] In human, no electroretinogram (ERG) responses were observed after *RPE65* gene transfer, whereas similar doses in dogs deficient for the same gene led to clinical responses, such as recovery of retinal activity and vision-guided mobility.[21,28] To note, dogs injected with suboptimal doses also showed improvement of visual behavior without ERG amelioration.[22,29] These discrepancies between clinical observations and animal studies raised concerns over viral vector efficacy in humans. Taking into account the data generated by Bainbridge et al. (2015), a 200-fold increase in gene expression could be necessary in humans to reach similar therapeutic effects as in canine models.[19,22]

In this context, the development of optimized vectors is a necessary step to improve gene expression after gene transfer. We previously investigated the efficacy of lentiviral vectors (LVs) for RPE65 gene transfer in rodent models, and showed the rescue of 100% of cones in the treated area of *Rpe65* knockout mice[30] and the reactivation of cone cellular function during the course of degeneration in *Rpe65*$^{R91W/R91W}$ mice,[31] an effect not reported so far. To further progress toward the clinical application of LVs for RPE65 deficiency, we have evaluated a GMP (Good Manufacturing Practice)–like production of an LV expressing the hRPE65 gene under the hRPE65 promoter,[30] injected subretinally into the eyes of nonhuman primates (NHPs). No systemic adjuvant anti-inflammatory prophylaxis was administered, contrary to other safety studies performed in large animals,[21,28,32-34] to detect potential side effects not observed in rodents that may occur when translating this gene therapy to primates.

The aim of this study was to evaluate the ocular and systemic safety of this LV following subretinal administration, in terms of retinal structure, retinal function, and systemic biodistribution.

METHODS

Animals and study design. This safety study on 5 naïve female *Macaca fascicularis* (3–6 years old), adhered to the ARVO Statement for the Use of Animals in Ophthalmic and Vision Research and obtained an institutional permission from the French Ministry of Agriculture after evaluation by the local ethical committee (2015062915001228vl). All procedures were performed in an approved user establishment (agreement number 92-032-02), in compliance with the European directive 2010/63/UE and French regulations. Animals were socially housed, had access to standard certified commercial primate food (Altromin, Genestil, Royaucourt, France) and processed municipal tap water, with food supplements such as fresh fruits. Room temperature was maintained at 20°C–24°C, with 55 ± 10% humidity and 12/12 light-dark cycle. Psychological and environmental enrichment was provided. Animals were regularly checked for clinical signs or other changes by caretakers and examined by the veterinary staff when needed.

To reduce the number of animals used in the study, and according to existing reports indicating an absence of systemic inflammatory reaction following

Table I. Description of eyes receiving the LV-RPE65 lentiviral vector or the vehicle (TSSM), in 5 female *Macaca fascicularis*

Monkey ID	Eye	Group	Time of sacrifice	Comments
1A	RE	TSSM	30 d after RE/LE injection	
	LE	LV-RPE65 dose 1		Injected same day as RE
1B	RE	LV-RPE65 dose 1	30 d after RE injection	
	LE	-		
2A	RE	TSSM	90 d after LE injection	
	LE	LV-RPE65 dose 2		Injected 30 d after RE
2B	RE	TSSM	90 d after LE injection	
	LE	LV-RPE65 dose 2		Injected 30 d after RE (1 accidental intravitreal dose + 1 subretinal dose)
C	RE	TSSM	90 d after RE injection	
	LE	-		

Abbreviations: LE, left eye; *RE*, right eye.

subretinal injection of TSSM, 3 NHPs received the LV solution (LV-RPE65) in one eye and the vehicle (TSSM) in the other eye. The fourth NHP received LV-RPE65 only in one eye and the fifth NHP received the vehicle only in one eye, this latter serving as negative control for the systemic biodistribution study (Table I). Two NHPs received a dose 1 of LV-RPE65 solution (2.8×10^5 IU in 100 μL; animals 1A and 1B), estimated to yield approximately one infectious particle per RPE cell in the detached retinal area and 2 other NHPs received LV-RPE65 at dose $2 = 10 \times$ dose 1 (2.8×10^6 IU in 100 μL; animals 2A and 2B). After the last clinical evaluation time point corresponding to the date of scheduled death, animals were sacrificed by intravenous injection of sodium pentobarbital and eyes and other organs were sampled.

Lentiviral vector production. The LV-RPE65 LV solution used in this study is a GMP-like production of a vector whose recombinant genome is similar to the one evaluated previously in RPE65-deficient mice.[30,31,35] Briefly, the LV-RPE65 is an integrative, third-generation, replication-defective, self-inactivating human immunodeficiency virus (HIV)-1–derived LV, with a mutated Woodchuck hepatitis virus Posttranscriptional Regulatory Element (WPRE) sequence devoid of promoter activities or open-reading frames.[36] It contains the R0.8 promoter (800 bp of the human RPE65 promoter)[28,37] which drives directly the expression of the RPE65 cDNA (without introns). For this study, we used the human RPE65 cDNA, while the mouse RPE65 cDNA was used previously to demonstrate vector efficacy in RPE65 mouse models.[30,31,35]

The RPE65 LV (LV-RPE65) was produced by transient transfection of suspended HEK293 T cells in a serum-free media (customized F17 medium, Invitrogen, Carlsbad, Calif), in a 10-L glass bioreactor (Biostat B-DCU, Sartorius, Göttingen, Germany). Briefly, LV-RPE65 was produced by transient 4-plasmid transfection with polyethylenimine (PEIpro, Polyplus-transfection, Illkirch-Graffenstaden, France) as transfection reagent. To enhance viral production, sodium butyrate was added 24 hours after transfection at a final concentration of 10 mM. To remove contaminating DNA a benzonase/Dnase solution (50 U/mL) was added 24 hours after transfection in the culture media. The cell supernatant was harvested 48-hour after transfection and filtered through 20/3/0.45-μm filters to discard cell debris and purified by following pre-GMP guidelines. The downstream purification process included an ion exchange chromatography, a concentration using a tangential flow filtration in a hollow fiber with 750-kDa cutoff (GE Healthcare, Little Chalfont, UK) and a final formulation in TSSM buffer (tromethamine 20 mM, NaCl 100 mM, sucrose 10 mg/mL, and mannitol 10 mg/mL).

Subretinal administration of LV or vehicle. Surgical procedures were performed after an overnight fasting period under general anesthesia with tracheal intubation and maintenance of spontaneous breathing. Anesthesia was induced by intramuscular ketamine chlorhydrate (100 mg/ml; 0.4-0.8 ml) and xylazine (20 mg/ml; 0.1-0.15 ml), followed by continuous intravenous propofol infusion (10 mg/ml; 1 ml then 3-5 ml/h).

All surgeries were performed by an experienced vitreoretinal surgeon (FBC) using a 3-port, sutureless pars plana vitreoretinal surgery system with valved 25-gauge trocars (Constellation, Alcon Laboratories, Inc, Fort Worth, Tex), after pupil dilation with tropicamide 1% and double povidone iodine disinfection of periocular skin, eyelids, and conjunctiva. The infusion line was placed inferotemporally, the left superior port was used for the light fiber and the right superior port for the injection cannula. A 41-gauge 'De Juan'

Cannula (Synergetics, Inc, O'Fallon, Mo) was used for subretinal injections. To minimize dead volume, it was connected via a custom low-caliber line to a 100-μL Hamilton Syringe (Sigma-Aldrich, St. Louis, Mo). Subretinal injections were performed at a site superior to the macula and adjacent to the superior arcade to obtain a macular detachment. No prophylactic systemic anti-inflammatory treatment was administrated before or at the time of the procedure. After injections, eyes received a single application of dexamethasone/oxytetracycline ointment. In one case of intense intraocular inflammation during the first postoperative week, anti-inflammatory treatment by intravenous or intramuscular methylprednisolone 1 mg/kg was administered daily during 3 days.

Clinical evaluation and multimodal retinal imaging. At each clinical evaluation time-point, anesthesia was performed similarly as for surgical procedures. Urine ($\sim$150 μL), venous blood ($\sim$150 μL), and tears ($\sim$20–50 μL) were sampled for viral particle shedding assays at days 0, 2, 4, 7, 14, and 28 in all animals, and additionally at day 90 for animals 2A, 2B, and C. Intraocular pressure (IOP) was measured using the iCare rebound tonometer (Icare Finland Oy, Vantaa, Finland). After pupil dilation with tropicamide 1%, the degree of intraocular inflammation was assessed by a trained ophthalmologist by grading the density of cells in the anterior chamber and vitreous in a 1 $\times$ 1-mm focused slit-lamp beam with 25 $\times$ magnification: 0 (no cells), 1+ (5–10 cells), 2+ (10–25 cells), 3+ (25–50 cells), and 4+ (>50 cells).

The fundus was assessed by indirect fundoscopy and fundus color photograph with the Smartscope camera (Optomed, Oy, Oulu, Finland). Optical coherence tomography (OCT), infrared reflectance, short-wavelength autofluorescence, and blue reflectance imaging were performed on Spectralis (Heidelberg Engineering, Heidelberg, Germany). If needed, fluorescein and indocyanine green angiography were additionally performed using Spectralis.

Optical coherence tomography analysis. Serial horizontal and vertical 30-degrees OCT sections acquired at the level of the fovea were processed using the automated layer segmentation tool of the Spectralis software (Heidelberg Eye Explorer, version 1.9.10.0) to obtain the layer thickness profiles for the total neurosensory retina (from internal limiting membrane to RPE), the outer nuclear layer (ONL, from its interface with the outer plexiform layer to the outer limiting membrane, OLM), and the photoreceptor outer segments–RPE complex (POS + RPE, from OLM to RPE). In each scan, the mean thickness corresponding to the detached area of the retina was extracted and calculated using a custom algorithm on MATLAB (version 2015b, MathWorks, Natick, Mass). At each time point, the mean layer thickness was estimated within the detached area by averaging the thickness obtained from the horizontal and vertical OCT scans.

An additional segmentation of retinal layers was performed using the custom-made DiOCTA software for OCT raw data analysis as described previously,[38] over an identical area within the detached retina in all eyes. This 1-mm-diameter circular area was located 1.1 mm superior and 2.2 mm nasal to the fovea, using as horizontal reference a straight line from the optic disc center to the fovea (Supplementary Fig 1). The distance between the injection site and this area was at least 3 disc diameters.

Electrophysiology. The ERG recordings were performed in all animals 1 week before the surgical procedures (baseline), 16 days and 30 days after the procedure, and additionally 90 days after the procedure in animals 2A, 2B, and C. Anesthesia with tracheal intubation and spontaneous breathing was obtained by intramuscular ketamine chlorhydrate and intravenous medetomidine hydrochloride administrations. Animals were prepared and recorded in a dim light room as previously described.[39,40] A 10.2.55 version Visiosystem (Siem Bio-Médicale, Nîmes, France) was used to generate the flash stimuli, as well as to record and analyze the ERG responses. Binocular full-field ERGs were elicited with 2 photostimulators (source: achromatic LEDs) for background conditions and flash stimulations (maximum intensity: 1.9 log cds/m2). First, the cone system was tested in photopic conditions against a bright background (25 cd.m^{-2}) aimed at desensitizing the rod system during 10 minutes. Photopic responses were obtained with 9 decreasing intensities of a series of 15 white LED bright flashes stimuli (from 1.90 log cd.s.m^{-2} to $-$0.80 log cd.s.m^{-2}) delivered at 1.3 Hz (interstimuli interval of 769 ms) to determine the "I_{max}" intensity corresponding to the maximum b-wave amplitude (V max) observed at the saturation point of the luminance curve (maximum cone system response).[41,42] Following determination of the I_{max} at each time point, the flicker ERG responses were obtained with white flash stimuli of I_{max} intensity delivered at 30 Hz during at least 15 seconds. Then the light was switched off and the rod system tested in scotopic conditions. After 20 minutes of dark adaptation, scotopic responses were obtained in dark conditions with an average of 5 dim light flashes (intensity: $-$1.1 log cd.s.m^{-2}) delivered at 0.1 Hz temporal frequency, corresponding to 10-second interstimuli intervals. Two minutes after the last scotopic flash, in the same scotopic conditions, the combined rod-cone response was elicited with a unique I_{max} white flash.

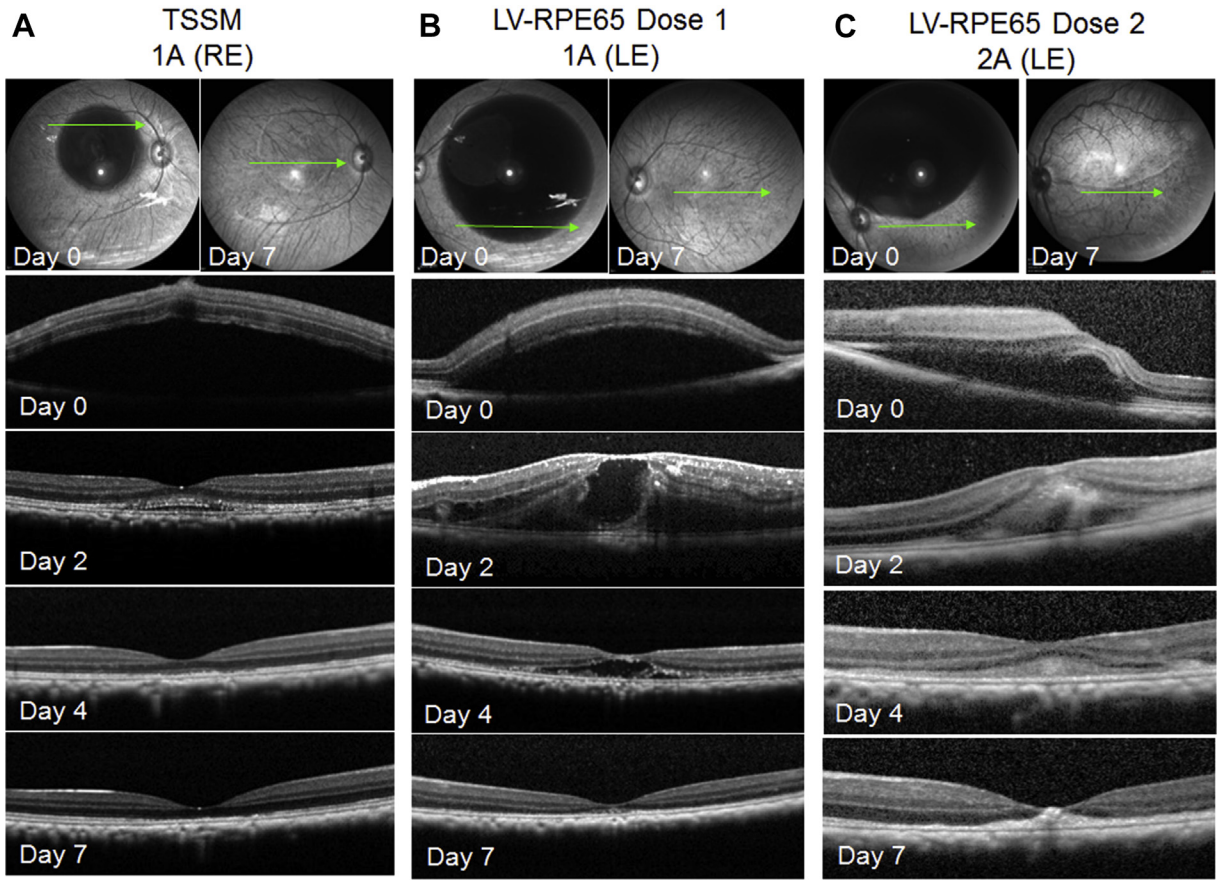

Fig 1. Course of progressive retinal reattachment after subretinal administration of vehicle or lentiviral vector preparation. In 3 representative eyes receiving the vehicle (TSSM, **A**), the LV-RPE65 lentiviral vector at dose 1 (**B**) or dose 2 (**C**), the upper panel shows infrared reflectance images immediately (left) and 7 days (right) after injection. Serial optical coherence tomography of the macula (green arrows) performed immediately and at days 2, 4, and 7 after administration show a progressive retinal reattachement. From the vehicle-injected eye to dose 1– and dose 2–injected eyes, there was an increasing reattachement delay and an increasing degree of early outer retinal alterations. LE, left eye; RE, right eye.

Assessment of shedding and distribution of LV particles. Shedding of lentiviral particles in body fluids (urine, blood, and tears) after injection was evaluated after RNA extraction of each fluid sample (NucleoSpin RNA Virus Kit, Macherey-Nagel, Düren, Germany) and storage at −80°C. Lentiviral particles were quantified by quantitative reverse transcriptase-polymerase chain reaction (qRT-PCR) targeting specific sequences of the lentiviral genome. Briefly, for each sample, 400 ng RNA were subjected to DNase digestion and reverse transcribed using SuperScript VILO cDNA synthesis kit (Life Technologies, Carlsbad, Calif) according to the manufacturer's instructions. The targeted transgene sequence was then amplified using iTaq universel SYBR Green Supermix on a CFX384 wells thermocycler (Biorad, Marnes-la-Coquette, France) with the following primers: forward primer, 5′-ATCCCTGTCACCTTTCATGG-3'; reverse primer, 5′-TGGGAATAAATGGCGGTAAG-3′ designed with Primer3 version 2.3.7 (http://sourceforge.net/projects/primer3). Samples and standard points were tested in duplicate.

The possible integration of lentiviral genome was assessed on genomic DNA extracted from flash frozen organ biopsies using the DNeasy blood and tissue kit (Qiagen, Hilden, Germany). DNA samples were stored at −20°C and processed for quantitative PCR targeting the human RPE65 mRNA sequence using the primer pair described above.

Ocular immunohistochemistry study. Enucleated eyes were fixed in 4% paraformaldehyde immediately after scheduled death procedures for 1 hour, then preserved in 1% paraformaldehyde, until they were equilibrated overnight in sucrose 30% and embedded in albumin from hen egg white (Fluka, Buchs, Switzerland). Sixteen-μm cryosections were obtained

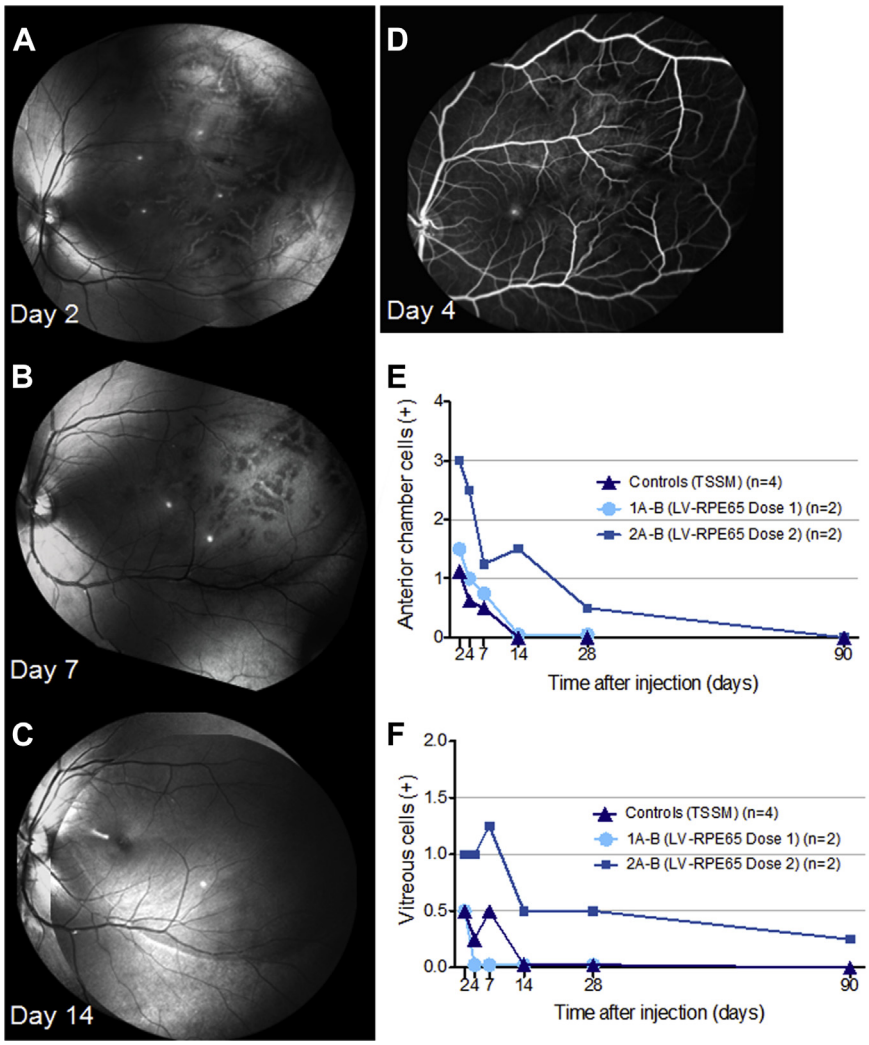

Fig 2. Assessment of ocular and retinal inflammation after LV-RPE65 subretinal injection. In (**A**) to (**C**) is displayed the Fundus blue reflectance imaging from the left eye of animal 1A, 2 days after the subretinal delivery of dose 1 LV-RPE65. (**A**) shows an early vasculitis-like perivenular reaction with progressive fading by day 7 (**B**) and resolution by day 14 (**C**). Fluorescein angiography in (**D**) performed at day 4 after administration did not reveal any active vasculitis. Anterior chamber cell count (**E**) showed a transient mild inflammation in TSSM- and dose 1–injected eyes and a more intense reaction in dose 2–injected eyes that resolved progressively over the course of follow-up. Similarly, vitreous cell count (**F**) showed a transient mild inflammation in TSSM- and dose 1–injected eyes and a moderately intense inflammation in dose 2–injected eyes that also resolved progressively over the course of follow-up. LE, left eye; RE, right eye.

from the temporal periphery to the optic nerve head. Immunohistochemistry was performed on macular and extramacular sections containing the injected area with antibodies directed against CD45 (#M0701, Dako, Zug, Switzerland), glial fibrillary acid protein (GFAP, #G3893, Sigma, Buchs, Switzerland), vimentin (#MA5-11883, Thermofischer Rockford, Ill), Iba-1 (#019–19741, Wako, Neuss, Germany), and M-Opsin (#AB5405, Chemicon, Temecula, Calif) which were revealed with the appropriate secondary antibodies coupled with Alexa Fluor488 (Molecular Probes, Eugene, Ore). Cryosections were also processed for hematoxylin-eosin stain.

Organ histology. Organ biopsies from inferior eyelids, right/left optic nerves, right/left geniculate bodies, right/left visual cortex, heart, liver, right/left lung, right/left ovary, right/left kidney, and right/left mandibular lymph nodes were obtained after sacrifice and transferred into formalin. After conventional tissue processing, evaluation for macroscopic/microscopic morphologic alterations and signs of inflammation

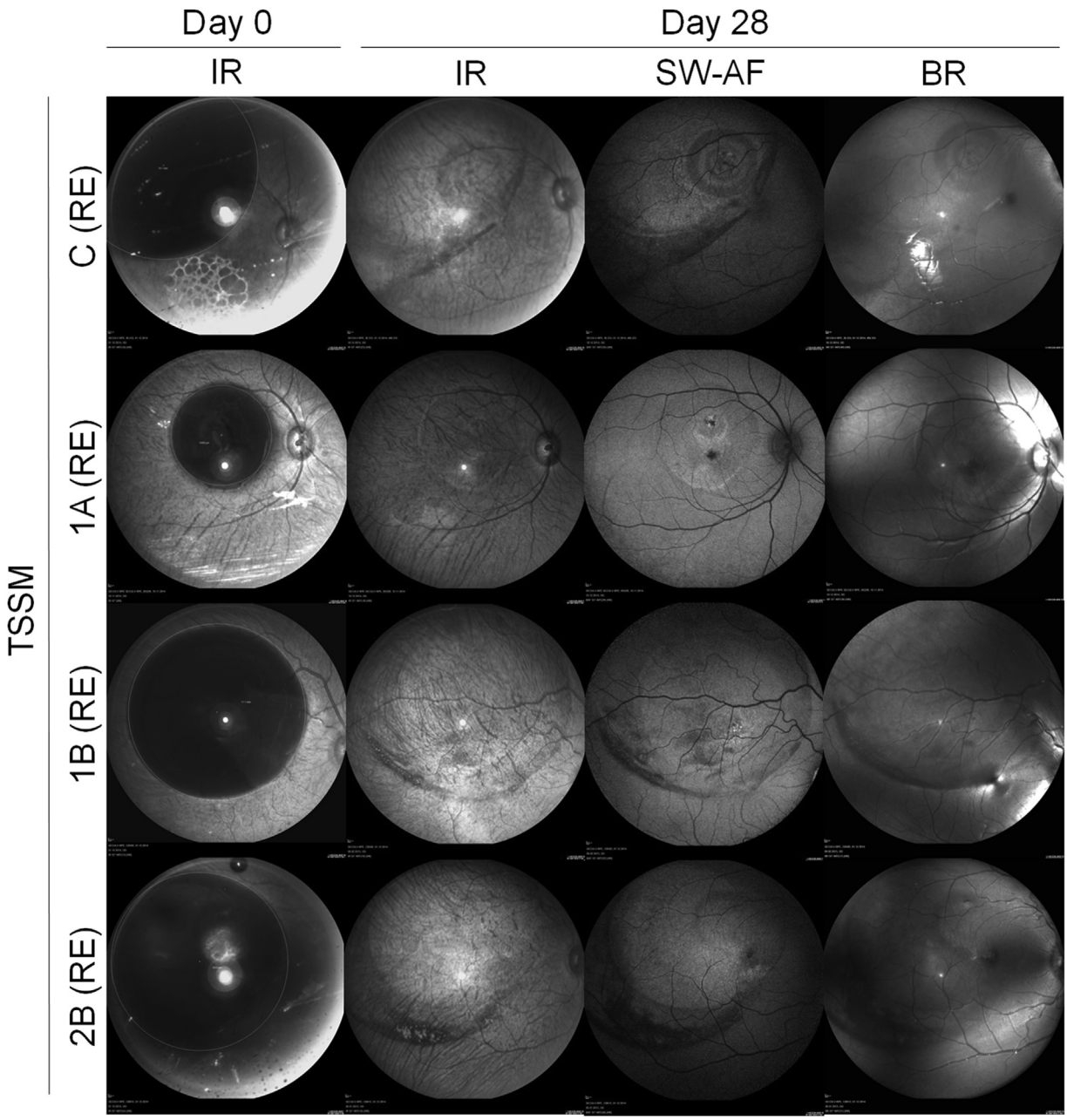

Fig 3. Multimodal imaging following subretinal administration of TSSM in 4 control *Macaca fascicularis* eyes. Infrared reflectance (IR) performed immediately after subretinal injection (day 0) showed the topography of the subretinal bleb, and revealed variable degrees of fundus pigmentary changes at day 28 after injection. Similarly, short-wavelength autofluorescence (SW-AF) and blue reflectance (BR) showed retinal pigment epithelium changes related to the detached retinal area or the injection site. Noticeably, the eye C (RE) exhibited a perifoveal concentric circular pattern in the 3 modalities, and the eyes C (RE), 1B (RE), and 2B (RE) showed a concentric hyporeflective and hypoautofluorescent ring at the periphery of the detached retinal area. LE, left eye; RE, right eye.

was performed by an experienced pathologist who was masked to group assignment.

RESULTS

Subretinal administration of LV-RPE65 vector and vehicle. A subretinal detachment of the macular area was obtained in all the 8 injected eyes (TSSM: 4 eyes; LV-RPE65 dose 1: 2 eyes; and LV-RPE65 dose 2: 2 eyes). The mean detached surface was 119 ± 4.2 mm^2 among the 4 eyes injected with LV-RPE65, showing good reproducibility for the delivery process. In the left eye (LE) of animal 2B

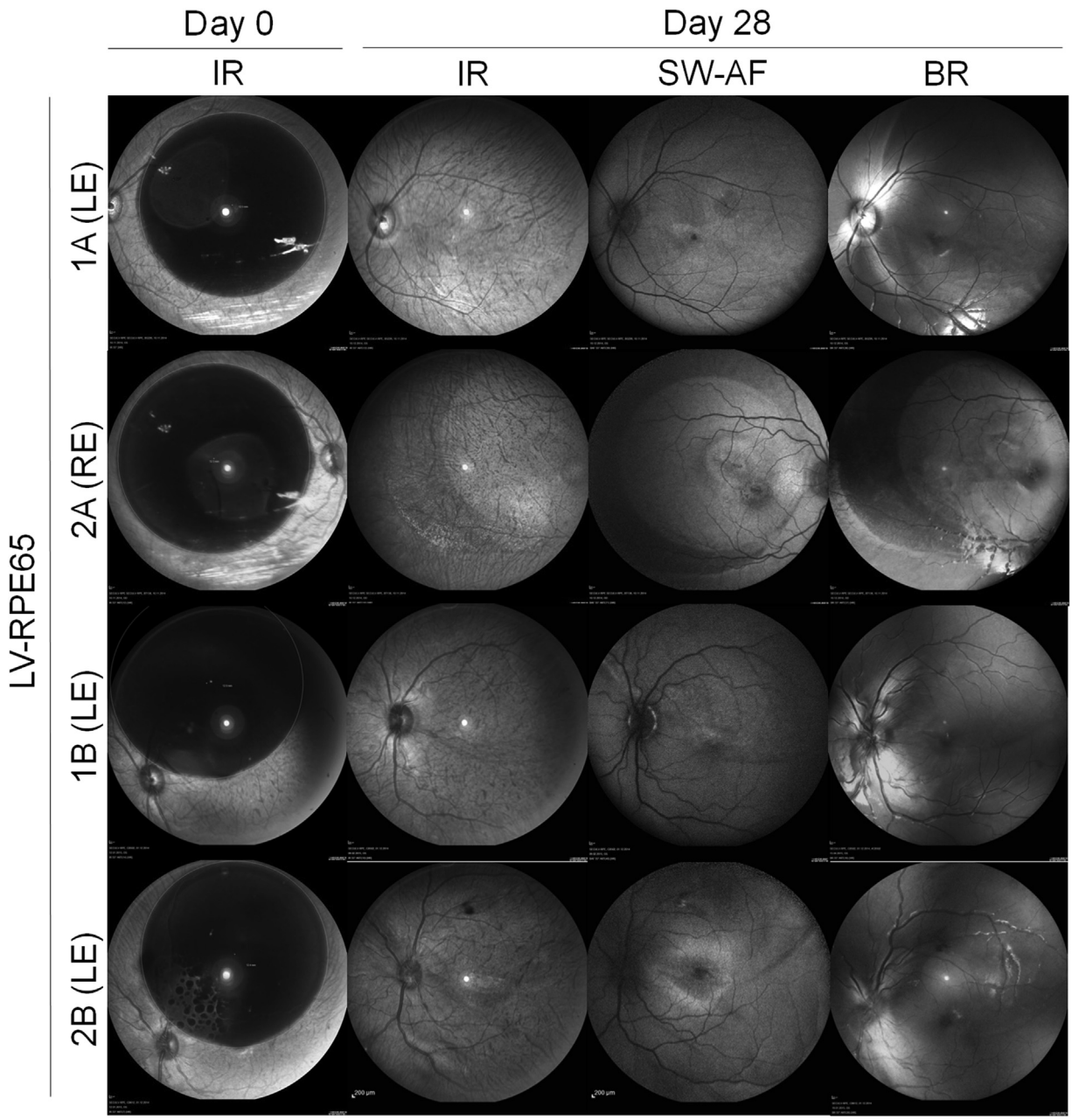

Fig 4. Multimodal imaging following subretinal administration of LV-RPE65 in 4 control *Macaca fascicularis* eyes. Infrared reflectance (IR) performed immediately after subretinal injection (day 0) showed the topography of the subretinal bleb and revealed mild fundus pigmentary changes at day 28 after injection. Similarly, short-wavelength autofluorescence (SW-AF) and blue reflectance (BR) showed moderate retinal pigment epithelium changes related to the detached retinal area or the injection site. Particularly, the 2A (RE) eye showed a concentric peripheral ring similar to those observed in TSSM-injected animals (Fig 3). The 2 B (LE) eye that received an additional intravitreal dose of LV-RPE65 presented a macular hyperautofluorescence suggestive of more advanced alterations of the outer retina and retinal pigment epithelium. By day 28, BR imaging showed no residual signs of the early, vasculitis-like reaction displayed in Fig 2. LE, left eye; RE, right eye.

(LV-RPE65 dose 2), the first attempt resulted in a retrohyaloidal injection with dispersion of the lentiviral solution within the vitreous cavity, and was followed by a second successful subretinal injection resulting in a 121-mm^2 bleb. OCT and fundus infrared reflectance images showing blebs immediately after injection are displayed in Figs 1–3, respectively.

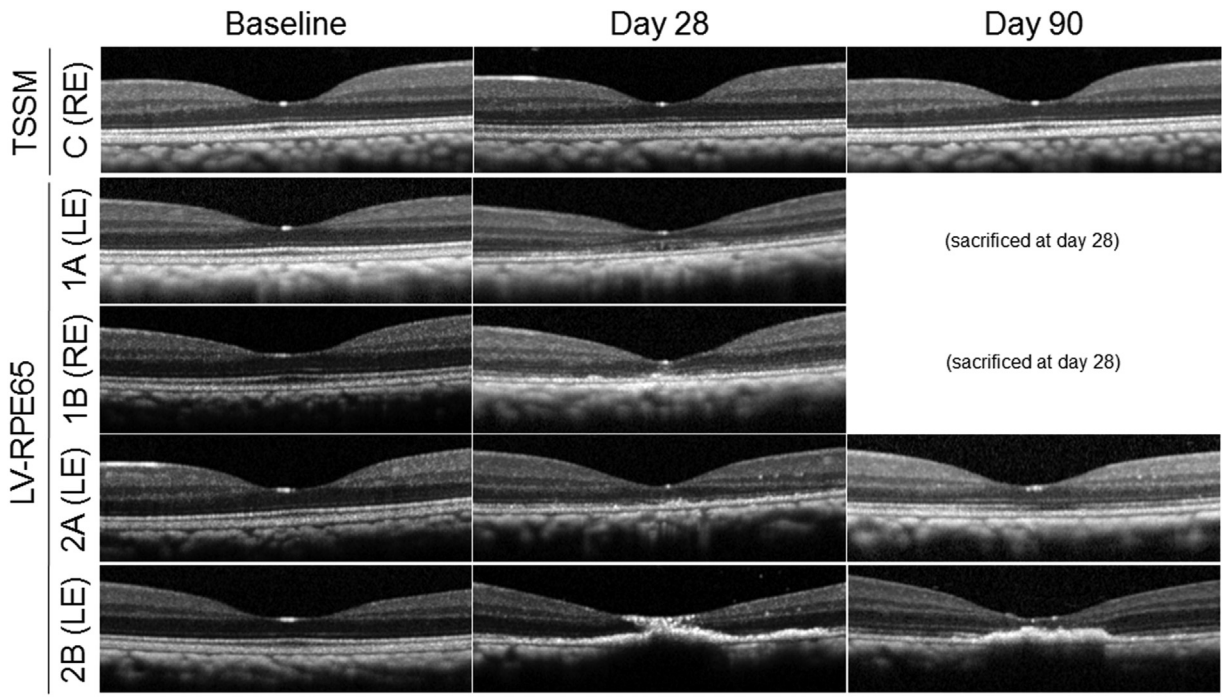

Fig 5. Optical coherence tomography of the fovea after subretinal administration of the LV-RPE65 lentiviral vector or the vehicle (TSSM). Horizontal optical coherence tomography scans at baseline (before subretinal administration), day 28, and day 90 (when available) showed minimal, reversible outer retinal changes with ellipsoid zone hyporeflectivity in one TSSM-injected eye (C [RE]). There was mild outer retinal alterations by day 28 in eyes receiving dose 1 LV-RPE65 (1A [LE], 1B [RE]), for which no imaging was available by day 90 due to earlier sacrifice in the study design. Similarly, there were moderate changes with a granular appearance of the ellipsoid zone in one dose 2 LV-RPE65–injected eye (2A [LE]), with recovery of ellipsoid zone integrity by day 90, but there was more pronounced outer retinal alterations with the presence of an hyperreflective material in the other LV-RPE65–injected eye (2B [LE]), that also received an accidental intravitreal dose of lentiviral vector. LE, left eye; RE, right eye.

Systemic assessment. A moderate weight loss was observed in 2 LV-RPE65–injected NHPs at the 30-day time point (animal 1A: −0.34 kg, animal 2A: −0.52 kg) that had resolved by 90 days for the animal that reached this time point (2A). Animal C who was dosed subretinally with TSSM only also presented a transitory weight loss (−0.41 kg) at 30 days that had resolved by 90 days. There were no unscheduled deaths during the study period.

Clinical and imaging ocular observations. The evaluation of subretinal blebs by serial OCTs during the first postoperative week showed a progressive reattachment that was completed at the fovea by day 4 in TSSM-injected eyes, and by day 7, at the latest, in LV-RPE65 dose 1–injected eyes. LV-RPE65 dose 2–injected eyes showed persistence of subretinal material at day 7, as illustrated in Fig 1, *B* and *C*.

Two days after subretinal injection, biomicroscopy revealed a moderate-to-intense anterior chamber and vitreous cellular reaction, which slowly resolved over the follow-up period. This reaction was more intense in dose 2–injected eyes than in dose 1– and vehicle-injected eyes (Fig 2, *E* and *F*). In particular, the LE of animal 2B which had received an extra intravitreal dose of LV-RPE65 presented initially an intense anterior chamber reaction (4+), requiring an intravenous dose of methylprednisolone, followed by progressive resolution of the intraocular reaction.

Surprisingly, all 4 eyes receiving LV-RPE65 presented an early vasculitis-like reaction with perivenular whitening and blood extravasation, suggestive of frost-branch angiitis. There was no sign suggestive of retinal necrosis, and the retinal signs subsided progressively over 14 days (Fig 2). This reaction was best recorded on fundus blue reflectance, indicating its localization to the inner retina around middle-sized retinal venules. Fluorescein and indocyanine green angiography performed at day 2 (animals 2A and 2B) or day 4 (animals 1A and 1B) did not show signs of active vasculitis, pointing to the early and transitory timing of this phenomenon.

There were variable fundus pigmentary changes in TSSM- and LV-RPE65–injected eyes, as illustrated in Figs 3 and 4. A circular hyperpigmentation was frequently visible at the periphery of the detached

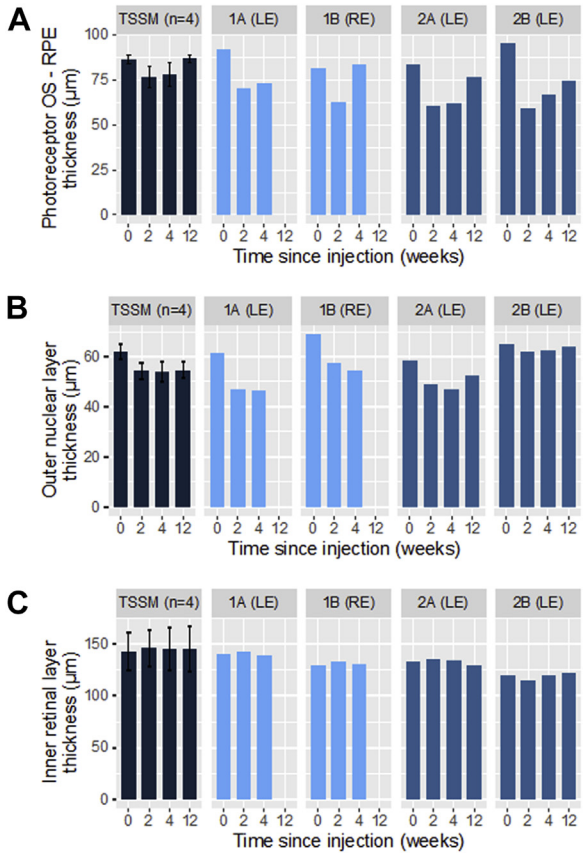

Fig 6. Changes in retinal layer thickness following subretinal administration of LV-RPE65 or the vehicle (TSSM). Retinal layer thicknesses were computed as the mean thickness within the detached area, along one vertical and one horizontal axis through the fovea. They are reported for 4 TSSM-injected control eyes (values pooled as mean ± SD, dark blue), and 4 LV-RPE65–injected eyes receiving dose 1 (animals 1A left eye, and 1B right eye, pale blue) or dose 2 (animals 2A left eye, and 2B left eye, mid-blue). (**A**) represents photoreceptor outer segment-retinal pigment epithelium thickness. An initial thinning was observed in control eyes dosed with TSSM, and in eyes receiving LV-RPE65 where it was more pronounced, with progressive recovery of photoreceptor outer segment-retinal pigment epithelium thickness over the follow-up. In the eye 2B (LE) that inadvertently received an extra intravitreal high dose of LV-RPE65 during administration procedure, a significant residual thinning persisted at day 90. (**B**) Quantification of the outer nuclear layer thickness shows an initial thinning effect and partial resolution in LV-RPE65–injected eyes evaluated at day 90. Control eyes receiving TSSM showed a milder outer nuclear layer thinning, which remained stable until day 90. (**C**) Inner retinal layers thickness, from the internal limiting membrane to the interface of the inner nuclear/outer plexiform layers, did not show major significant variation. Thickness of inner retinal layers was very close to baseline values by days 28 and 90 in TSSM-injected and LV-RPE65 injected eyes. LE, left eye; RE, right eye.

area, with a clear hyperpigmented ring in 3 TSSM-injected and 1 LV-RPE65–injected eye, visible on infrared and blue reflectance, and short-wavelength autofluorescence. There was also hypo/hyperautofluorescent changes related to the injection site, and a pattern formed by multiple concentric rings variably observed around the fovea.

A transient decrease in IOP was observed in all eyes after surgery, and was more pronounced in LV-RPE65–injected eyes than TSSM-injected eyes, probably related to the degree of postoperative intraocular inflammation. However, it was self-resolving with mean IOP measurements of 10-mm Hg, 8-mm Hg, and 11-mm Hg at day 28 in eyes dosed with LV-RPE65 dose 1, dose 2, and TSSM, respectively.

Assessment of retinal layers on OCT. The qualitative evaluation of retinal layers at the macula with serial OCT showed outer retinal changes at day 28 in LV-RPE65–injected eyes (Fig 5). The ellipsoid zone (EZ) demonstrated an irregular aspect in eyes 1A (LE), 1B (right eye [RE]), and 2A (LE), while the hyperreflective material observed after bleb formation (Fig 1) persisted in the LE of animal 2B, impairing the visualization of outer retinal layers at the macula. The ONL also showed a relative thinning in eyes dosed with LV-RPE65. At the 90-day time point, eye 2A (LE) showed a partial restoration of EZ, and eye 2B (LE) showed a partial regression of the dense hyperreflective material, and persistence of outer retinal layer alterations. EZ disruption and ONL thinning were also observed, but to a milder degree, in eyes dosed with TSSM (Fig 5 shows OCTs from animal C [RE]). For all groups but not for all animals, accumulation of subretinal hyperreflective material was observed at the bleb edge (not shown).

A quantitative assessment of retinal layer thickness changes on OCT scans positioned at the fovea in detached retinal areas is displayed in Fig 6. It showed in LV-RPE65–injected eyes a transient, partially reversible POS-RPE layer thinning. The ONL thickness was also moderately affected. To a lesser degree, outer retinal layer thicknesses in control TSSM-injected eyes were also altered by the subretinal detachment, and demonstrated similar trends with reversible outer segment thinning and a moderate, persistent ONL thinning in the detached area. A similar assessment was performed for the inner retinal layers (from the internal limiting membrane to the outer plexiform/inner nuclear layer interface), that showed no relevant thickness changes in TSSM-injected and LV-RPE65–injected eyes.

An analysis of retinal layer thickness change was also conducted over an identical location close to the macula in all eyes,[38] allowing a better intereyes comparability of the results in terms of relative change. This analysis showed a reversible decline in ONL thickness and a relative, partial decrease in POS/RPE thickness in all

LV-RPE65–injected eyes (Supplementary Fig 2). It also confirmed that the inner retinal layer thickness was not modified after LV-RPE65 injection.

Electroretinography. To evaluate the effects of subretinal administration of either LV-RPE65 or TSSM on retinal activity, we compared full-field ERG recordings performed 14, 28, and 90 days after injection with baseline measures acquired before treatment, in each animal (Table II). Baseline responses showed evident interindividual quantitative variations of the a- and b-wave amplitudes. For example, min-max values ranged from 40 to 108 μV for the b-wave amplitude of the rod response or from 22 to 49 μV for the a-wave amplitude of the cone response. We thus decided to evaluate intraindividual variations at the different time points. Of the 4 TSSM-injected eyes, 3 eyes maintained equivalent retinal activity (Fig 7*B*). In the fourth TSSM-injected eye C (RE), we observed over 40% decrease in response amplitudes to all illumination conditions after injection as compared to baseline, but no differences in peak times. Absent or minor modifications of ERG responses were noticed for the 2 LV-RPE65–injected eyes 1B (RE; dose 1) and 2A (LE; dose 2; Fig 7, *C* and *D* and Table II), whereas the 1A (LE) dose 1 showed significantly reduced amplitudes at the latest time point by 40% or more, but without peak time increase. The fourth eye injected with LV-RPE65 dose 2 (2B [LE]) showed 90 days post-injection both reduced amplitude and increase in peak time in scotopic conditions, which could be the manifestation of retinal cellular suffering (Table I). We were not able to identify exclusive inner retinal dysfunction in LV-RPE65– or TSSM-injected eye following ERG analysis of a- and b-wave amplitudes and peak times.

Biodistribution and organ toxicology. To optimize quantitative PCR sensitivity for detecting circulating lentiviral particles or integrated lentiviral genomes, we designed a primer pair targeting specifically the lentiviral transgene cassette. The forward primer is located on RPE65 cDNA and the reverse primer on the Woodchuck hepatitis virus Posttranscriptional Regulatory Element sequence added in the vector, thereby avoiding putative amplification of the endogenous *RPE65* macaque gene. This primer pair allowed to detect unequivocally 10 copies of target matrix DNA in the reaction mixture (Supplementary Fig 3).

Circulating particles. To evaluate the extraocular shedding of lentiviral particles after subretinal delivery, qRT-PCR was performed on lachrymal fluid, serum, and urine collected at regular intervals (days 2, 4, 7, 14, 30, and 90). Based on the sensitivity of the qPCR and the amount of RNA extracted from the different fluids, we calculated a detection threshold of 250 particles/ml for serum, 60 particles/ml for lachrymal fluid, and 10 particles/ml for urine. No viral particle was detected in any body fluid regardless the time points or the animal being studied all quantification cycles (Cq) being equivalent or above negative control (Supplementary Fig 3).

Integrated lentiviral sequences in genomic DNA. Despite the very limited shedding of the vector, we prospected for extraocular genomic integration of the LV. Biopsies from inferior eyelids, right/left optic nerves, right/left geniculate bodies, right/left visual cortex, heart, liver, right/left lung, right/left ovary, right/left kidney, and right/left mandibular lymph nodes were collected at the end of the experiment and genomic DNA was extracted for quantitative PCR of the integrated therapeutic cassette. The threshold sensitivity of our procedure was 10 copies in 50 ng of genomic DNA, the lowest detected point of the standard curve being 10 copies. This limit of detection was estimated to be at 0.8×10^6 copies/organ for heart (containing around 4.9×10^{14} diploid genomes), 1×10^6 copies/organ for lung (containing around 6.8×10^{14} diploid genomes), 2×10^6 copies/organ for kidney (containing around 15.8×10^{14} diploid genomes), 12×10^6 copies/organ for liver (containing around 76.5×10^{14} diploid genomes), and brain (containing around 75.8×10^{14} diploid genomes). We did not detect any integration of the recombinant lentiviral genome in any samples tested showing the systemic safety of lentiviral administration into the subretinal space.

Organ histology. No macroscopic or microscopic morphologic alterations nor signs of unexpected inflammation could be detected in biopsies sampled from inferior eyelid, optic nerve, geniculate bodies, visual cortex, mandibular lymph node, heart, lung, liver, kidney, and ovary tissues in animals sacrificed at day 28 (1A-B) or day 90 (2A-B) after LV-RPE65 subretinal administration nor in the animal sacrificed 90 days after receiving TSSM only (C).

Ocular histology and immunohistochemistry. After sacrifice at day 28 for dose 1 LV-RPE65–injected animals and at day 90 for dose 2 LV-RPE65–injected animals, eyes were processed for histologic and immunohistochemical analysis. Conventional hematoxylin-eosin stain showed normal ocular structures in all eyes and revealed a mild choroidal lymphocytic infiltrate in animal 1A (RE; TSSM), and a similar finding associated to focal outer blood-retinal barrier breakdown and mild vitritis in animal 2B (LE; LV-RPE65 dose 2). To evidence remnants of inflammatory cell migration, a retinal section containing the region of subretinal injection (bleb) was labeled for the CD45 leukocyte marker. No differences in CD45-positive labeling were observed between noninjected, TSSM-injected, or LV-RPE65–

Table II. Retinal activity characterization using full field electroretinogram (ERG) recordings following subretinal injection

				Photopic (cone responses) at i-max 0.4 log cds/m^2						Scotopic (rod responses) at −0.8 log cds/m2		Scotopic (mixed rod-cone responses) at i-max 0.4 log cds/m^2				
				a-wave		b-wave			Fl-wave	b-wave		a-wave		b-wave		
ID	Eye	Group	Time	Amp (μV)	Peak time (ms)	Amp (μV)	Peak time (ms)	Ratio b/a	Amp (μV)	Amp (μV)	Peak time (ms)	Amp (μV)	Peak time (ms)	Amp (μV)	Peak time (ms)	Ratio b/a
C	LE	-	Baseline	47	14	205	31	4.36	190	92	60	145	16	367	38	2.53
			D15	34	14	137	30	4.03	123	54	62	100	17	243	39	2.43
			D30	33	14	136	30	4.12	129	55	61	98	16	254	38	2.59
			D90	22	14	134	29	6.09	128	61	61	105	17	285	38	2.71
1B	LE	-	Baseline	29	14	126	27	4.34	105	51	56	104	16	251	36	2.41
			D15	38	14	119	32	3.13	111	64	62	130	14	270	36	2.08
			D30	30	13	127	30	4.23	140	57	59	132	14	298	34	2.26
C	RE	TSSM	Baseline	49	14	213	30	4.35	186	93	60	147	16	382	38	2.60
			D15	30	15	125*	30	4.17	94*	46*	64	97	17	214*	41	2.21
			D30	22*	14	105*	30	4.77	96*	34*	60	79*	16	194*	39	2.46
			D90	23*	15	107*	29	4.65	96*	42*	61	86*	17	224*	38	2.60
1A	RE	TSSM	Baseline	32	14	153	29	4.78	109	54	60	119	17	287	40	2.41
			D15	41	13	158	28	3.85	130	75	60	144	16	346	38	2.40
			D30	22	15	122	29	5.55	69	44	58	109	17	240	41	2.20
2A	RE	TSSM	Baseline	25	13	149	27	5.96	144	88	55	110	16	360	39	3.27
			D15	35	14	150	29	4.29	120	84	57	107	16	332	39	3.10
			D30	32	13	168	27	5.25	172	118	53	134	15	454	40	3.39
			D133	29	13	137	27	4.72	131	79	53	97	15	299	40	3.08
2B	RE	TSSM	Baseline	25	13	109	27	4.36	107	65	57	107	15	305	35	2.85
			D15	38	12	116	32	3.05	148	64	60	138	13	320	35	2.32
			D30	43	11	140	32	3.26	181	89	57	152	14	387	34	2.55
			D133	29	13	112	28	3.86	101	60	61	104	16	266	38	2.56
1A	LE	Dose 1	Baseline	32	12	160	29	5.00	129	61	61	130	17	302	40	2.32
			D15	28	14	112	28	4.00	166	53	62	102	16	230	39	2.25
			D30	19*	15	91*	29	4.79	53*	27*	59	83	17	194	42	2.34
1B	RE	Dose 1	Baseline	22	14	97	27	4.41	84	40	56	91	16	212	35	2.33
			D15	41	14	109	32	2.66	120	50	64	129	15	246	37	1.91
			D30	39	13	110	31	2.82	140	50	59	138	15	288	35	2.09
2A	LE	Dose 2	Baseline	27	13	163	27	6.04	163	108	54	113	15	400	40	3.54
			D22	22	13	111	28	5.05	105	73	55	91	16	305	40	3.35
			D30	20	14	120	28	6.00	105	82	57	93	16	293	42	3.15
			D90	16*	14	96*	28	6.00	93*	71	54	88	16	294	41	3.34
2B	LE	Dose 2	Baseline	36	13	139	27	3.86	151	83	57	129	15	365	35	2.83
			D22	29	13	140	29	4.83	97	67	64	115	17	286	41	2.49
			D30	38	14	123	32	3.24	120	54†	62†	131	16	318	38	2.43
			D90	19*	14	93	29	4.89	68*	51†	63†	79†	17†	213†	40†	2.70

*> 40% decrease compare to baseline.
†decrease of amplitude coupled to mild increase of peak time.

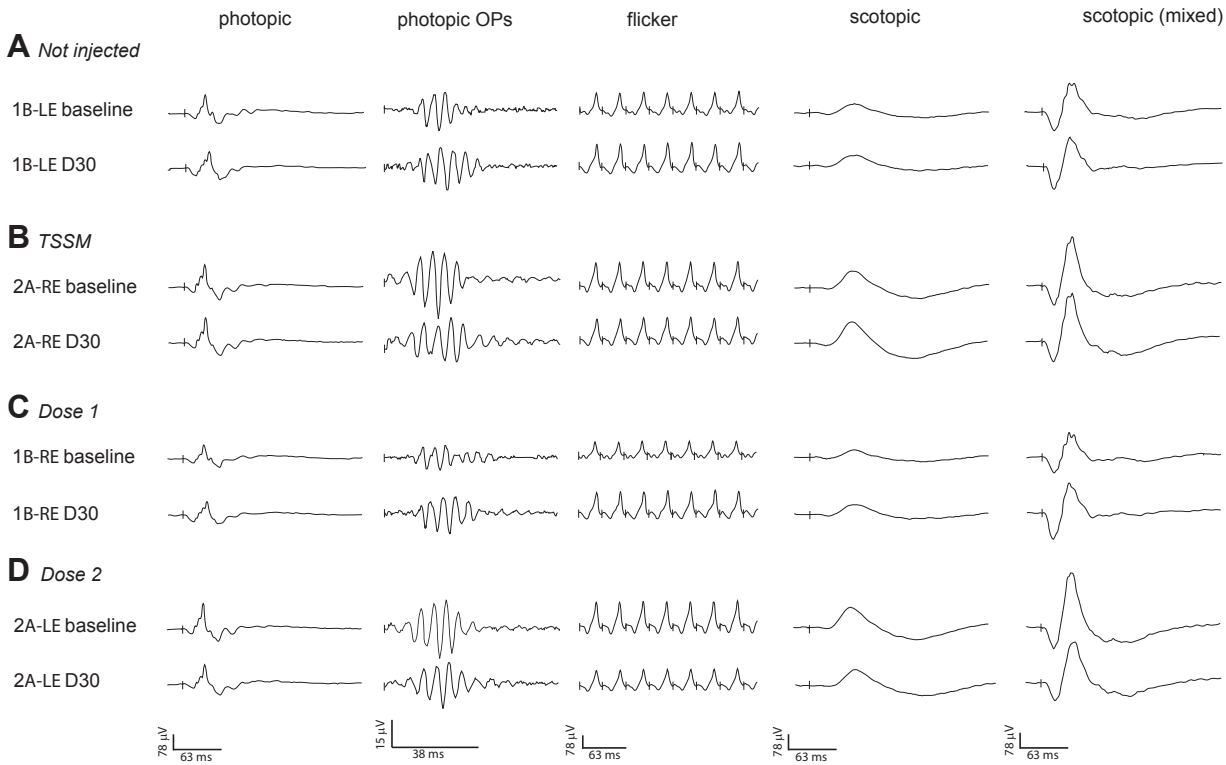

Fig 7. Retinal activity evaluation 30 days after subretinal injection. ERG tracings obtained at baseline and 30 days after injection in photopic and scotopic conditions. In photopic conditions, the I_{max} flash response was obtained by 15 stimuli delivered at 1.3 Hz against a 25 cd/m^2 background (first column). The oscillatory potentials were extracted from the I_{max} photopic response (second column). A final 30-Hz flicker at I_{max} stimuli was recorded (third column). After 20 minutes of dark adaptation, scotopic responses to 0.4 cd.s/m^2 stimuli (average of 5 flashes) were recorded in dark (fourth column). Finally, in similar scotopic conditions, a unique flash at I_{max} intensity was applied to record the mixed rod-cone response (fifth column). The displayed tracings were obtained in (**A**) an uninjected eye (1B [LE]), (**B**) a TSSM- injected eye (2A [RE]), (**C**) a dose 1 LV-injected eye (1B [RE]), and (**D**) a dose 2 LV-injected eye (2A [LE]). All eyes maintained photopic and scotopic retinal activity 30 days after injection. LE, left eye; RE, right eye.

injected eyes (Supplementary Fig 4). The GFAP and Vimentin glial markers labeling Müller cells and astrocytes did not show any difference between these eyes (Supplementary Fig 4). Finally, the microglia Iba-1 staining did not either demonstrate differences in microglial activation or migration between these groups 30 or 90 after injection (Supplementary Fig 4).

DISCUSSION

In this preclinical study, we assessed the ocular and systemic safety after subretinal administration of an LV for RPE65 gene replacement in healthy NHPs. Considering that no systemic or periocular anti-inflammatory agents were preventively administered to the subretinally injected animals, subretinal injection of an LV was well tolerated in low-dose injected animals, but not in the high-dose injected animals who developed a strong retinal and ocular inflammatory reaction, that did not persist but induced seemingly irreversible structural alterations. This observation suggests that the alterations observed at the fovea level could be markedly reduced if the injection procedure and the retina environment are well controlled. This moderate tolerance has to be compared with previous preclinical and clinical studies with AAV vectors, in which large animals or patients all received periocular[16,28,43] or systemic[18,33] anti-inflammatory therapy. An exception was made for animal 2B which endured an accidental intravitreous extra-injection and developed a marked, but transient intraocular inflammation and who received an intravenous anti-inflammatory treatment. This animal developed a mild transient weight loss, but this phenomenon was also observed in one TSSM-injected animal and might be caused by repetitive anesthesia imposed by the study design. Remarkably, no vector shedding or inaccurate extraocular targeting was demonstrated, showing the safe restriction of the vector

in the eye. This observation is consistent with previous reports suggesting a high systemic safety of nonhuman LVs administered subretinally.[44-47]

In the present study, in contrast with previous reports that did not focus on early events, animals were followed at short intervals with multimodal imaging to assess in vivo the acute effects of subretinal LV administration on retinal structures. Interestingly, the kinetics of subretinal bleb detachment showed prolonged reattachment times (by 3–4 days) for LV-RPE65–injected eyes as compared with vehicle-injected eyes. This phenomenon may be caused by a transient impairment of the RPE pumping capacity during an acute phase corresponding to the vector entry and integration into RPE cells, the latter process starting within 4 hours and reaching a plateau at 24–48 hours.[48] Alternatively, the transient presence of viral particles in the subretinal fluid could provoke an osmolality imbalance that maintains the detachment of the neurosensory retina from the RPE longer than in control-injected eyes. Whether this prolonged detachment results from the alteration of RPE cell functions in reaction to vector entry, from an inflammatory process, or from an osmolality effect remains to be determined.

Noticeably, we observed an early perivascular reaction, evidenced at day 2 and self-resolving within 14 days, consisting perivenular whitening at the level of retinal venules within the detached area. There was no angiographic vasculitis at day 2, suggesting that severe blood-retinal barrier rupture did not occur or occurred before this time point. Although a similar reaction has not been reported by other groups, we did not find previous reports of fundus examination or blue-reflectance imaging, which best evidenced the phenomenon, as early as day 2 after subretinal delivery of viral vectors. To investigate its cause, we searched for several inflammatory and glial markers by immunohistochemistry but did not find overexpression of CD45 (lymphocytes), Iba-1 (microglia), GFAP or vimentin (astrocytes and Müller cells) in LV-RPE65–injected as compared with vehicle-injected eyes. This may result in part from the delayed ex vivo evaluation at 1 and 3 months after administration. Nonetheless, these histologic data assess that this transient reaction did not provoke a chronic modification of the glial cells often observed after retinal injuries.[49,50]

Importantly, the in vivo evaluation of retinal layer thickness by serial OCT scans did not show any significant thinning of inner retinal layers, where the perivascular reaction was detected.

While the perivascular phenomenon occurred in all eyes receiving LV-RPE65, no significant ERG alterations were observed in all the 4 animals, indicating limited consequences on retinal function. Similarly, ERG alterations observed in LV-RPE65–injected eyes did not preferentially involve b-wave responses, suggesting that the immediate post-injection vasculitis-like process did not result in specific inner retinal cellular defects detectable by this analysis. Moreover, no isolated b-wave modifications were observed, suggesting they were rather caused by a-wave changes originating from outer retinal variations rather than from inner retinal damages.

Outer retinal alterations were also manifested on multimodal imaging as hyper/hypopigmentation, and hyper/hypoautofluorescence mostly at the borders of the detached areas. OCT also showed a partially reversible thinning of outer retinal layers. Similarly to ERG a-wave variations, these changes were more frequent and more severe in LV-RPE65–injected eyes, but were also observed to a variable and milder degree in vehicle-injected eyes. Despite the limited number of injected eyes (4 with TSSM, 2 with low-dose LV-RPE65, and 2 with high-dose LV-RPE65), these observations emphasize the limits of the subretinal route with current injection methods and devices that do not prevent retinal suffering, particularly at the POS/RPE interface, and that lack reproducibility. The crescent-shaped pigmentary and autofluorescent modifications visible on Figs 3 and 4 variably affected both vehicle- and lentivirus-injected eyes. This imaging pattern points to a biological effect of the retinal detachment rather than to an infectious manifestation. Moreover, although restoring a retinal function in the macular area should bring major benefits to the patients, this area appears to be especially vulnerable to the damaging effects of acute detachment, as was already highlighted in one clinical study evaluating AAV-based RPE65 gene therapy.[26] In the present study, 3 out of 4 animals presented at 1 or 3 months a partial improvement of early macular changes visible on OCT after LV-RPE65 administration. In contrast, animal 2B which received an extra intravitreal dose followed by an intense intraocular inflammation presented a subfoveal hyperreflective deposit that had not resolved at the 3-month time point, showing the higher susceptibility of the fovea for focal damage in case of an adverse event. Among patients included in AAV-RPE65 gene therapy clinical trials, structural damage of the fovea has been reported, such as macular hole formation[17] and foveal thinning,[22,23,26] To prevent these drawbacks, alternate strategies have been advanced, such as minimizing hydrodynamic stress during injection[51,52] or performing multiple perimacular detachments.[26]

Animal models of retinal detachment have shown that detachment of the neurosensory retina from the RPE leads to a glial reaction mediated by Müller cells[53,54] and microglia,[55] and to photoreceptor damage with outer segment shortening.[56] Photoreceptor damage results from

the activation of multiple pathways, including the alternative complement[57] and RhoA pathways.[58] Interestingly, there is a decrease in glial markers overexpression[59] and progressive restoration of POSs[56] after lengthy periods of reattachment (~5 months), which is consistent with our findings. Recently, imaging studies using OCT segmentation on patients with rhegmatogenous retinal detachment also showed a re-increase in POS volume after retinal reattachment.[60] In LV-RPE65–injected eyes, damages related to the induced retinal detachment may be potentiated by the inflammation reaction to the viral vector, explaining the less-pronounced photoreceptor restoration as compared with control eyes. However, multimodal imaging findings in the present study showed a variability in retinal alterations after subretinal administration of TSSM or the lentiviral solution, as reported in patients who received subretinal gene therapy.[22,26] Additional studies with increased number of vector-injected eyes will be necessary to demonstrate in greater detail the functional and structural effects of subfoveal injections.

The blood-retinal barrier, by contributing to the intraocular immune privilege, favors the systemic tolerance of subretinally injected vectors. However, mechanical alterations of the RPE induced by the detachment, and the transient perivascular reaction observed in this study may compromise the integrity of the outer and inner blood-retinal barriers, respectively. Although the analysis of body fluids and organs did not indicate shedding of viral particles, it may have elicited a subclinical, low-grade immune reaction, which raises concerns regarding possible vector reinjection.[43,61] The evaluation of the immune response against the LV-RPE65 vector will be addressed in a future report.

Limitations of this study include the limited number of NHPs due to ethical restrictions, and the fact that one animal was treated after surgery with systemic corticosteroids due to an intense intraocular inflammation. Additional experiments are needed to evaluate the dose safety, to determine whether vitrectomy should be performed systematically before subretinal injection, whether the injection site should be located in a specific area or sealed to reduce vitreal leakage of the vector, and whether local or systemic corticosteroids should be administered.

The current RPE65 clinical trials are proposing an AAV-based gene transfer for gene replacement in RPE cells. Despite positive effects in the first years following vector administration, several long-term reports show continuation of retinal degeneration, and loss of early visual benefits several years after treatment[22,23,62] One hypothesis explaining this major drawback is the low level of therapeutic gene expression obtained in these trials, which is incompatible with the level required in the human retina.[22] Thus, the development of alternate gene transfer tools could open new therapeutic perspectives.[19] Given the previously established high efficiency of LVs to target RPE cells,[30,31,63,64] this vector may be a potential candidate for inherited retinal disorders due to RPE65 deficiency, but also for other RPE-specific diseases such as Best vitelliform macular dystrophy, provided that its local tolerance is improved. This improvement may be achieved by the co-administration of a systemic adjuvant anti-inflammatory prophylaxis and/or optimization of the vector delivery. The study herein further supports the limited systemic dispersion of LVs following subretinal administration. It also demonstrates that further optimization of the retinal tolerance to the LV-RPE65 LV and to its subretinal delivery technique are crucial to render the vector eligible for gene transfer in the human retina.

ACKNOWLEDGMENTS

Conflicts of Interest: All authors have read the journal's policy on disclosure of potential conflicts of interest and have none to declare. This work was supported by SwissTransmed and the Fondation l'Occitane. The authors thank Solenne Métrailler and Damien Grize for technical assistance. The authors are also particularly grateful to José-Alain Sahel, Céline Jaillard, Elena Brazhnikova, Claire-Maëlle Fovet, Joanna Demilly, and Lev Stimmer for granting access to the animal facility and their assistance in animal experiments and to Charlène Joséphine for performing quantitative PCR experiments.

REFERENCES

1. Ali RR, Reichel MB, Thrasher AJ, et al. Gene transfer into the mouse retina mediated by an adeno-associated viral vector. Hum Mol Genet 1996;5:591–4.
2. Flannery JG, Zolotukhin S, Vaquero MI, LaVail MM, Muzyczka N, Hauswirth WW. Efficient photoreceptor-targeted gene expression in vivo by recombinant adeno-associated virus. Proc Natl Acad Sci U S A 1997;94:6916–21.
3. Bennett J, Maguire AM, Cideciyan AV, et al. Stable transgene expression in rod photoreceptors after recombinant adeno-associated virus-mediated gene transfer to monkey retina. Proc Natl Acad Sci U S A 1999;96:9920–5.
4. Bennett J, Tanabe T, Sun D, et al. Photoreceptor cell rescue in retinal degeneration (rd) mice by in vivo gene therapy. Nat Med 1996;2:649–54.
5. Smith AJ, Bainbridge JWB, Ali RR. Gene supplementation therapy for recessive forms of inherited retinal dystrophies. Gene Ther 2012;19:154–61.
6. Boye SE, Boye SL, Lewin AS, Hauswirth WW. A comprehensive review of retinal gene therapy. Mol Ther 2013;21:509–19.

7. Miyoshi H, Takahashi M, Gage FH, Verma IM. Stable and efficient gene transfer into the retina using an HIV-based lentiviral vector. Proc Natl Acad Sci U S A 1997;94:10319–23.
8. Bainbridge JW, Stephens C, Parsley K, et al. In vivo gene transfer to the mouse eye using an HIV-based lentiviral vector; efficient long-term transduction of corneal endothelium and retinal pigment epithelium. Gene Ther 2001;8:1665–8.
9. van Adel BA, Kostic C, Déglon N, Ball AK, Arsenijevic Y. Delivery of ciliary neurotrophic factor via lentiviral-mediated transfer protects axotomized retinal ganglion cells for an extended period of time. Hum Gene Ther 2003;14:103–15.
10. Balaggan KS, Binley K, Esapa M, et al. Stable and efficient intraocular gene transfer using pseudotyped EIAV lentiviral vectors. J Gene Med 2006;8:275–85.
11. Colella P, Auricchio A. Gene therapy of inherited retinopathies: a long and successful road from viral vectors to patients. Hum Gene Ther 2012;23:796–807.
12. Cideciyan AV. Leber congenital amaurosis due to RPE65 mutations and its treatment with gene therapy. Prog Retin Eye Res 2010;29:398–427.
13. Redmond TM, Yu S, Lee E, et al. Rpe65 is necessary for production of 11-cis-vitamin A in the retinal visual cycle. Nat Genet 1998;20:344–51.
14. Marlhens F, Bareil C, Griffoin JM, et al. Mutations in RPE65 cause Leber's congenital amaurosis. Nat Genet 1997;17:139–41.
15. den Hollander AI, Roepman R, Koenekoop RK, Cremers FPM. Leber congenital amaurosis: genes, proteins and disease mechanisms. Prog Retin Eye Res 2008;27:391–419.
16. Hauswirth WW, Aleman TS, Kaushal S, et al. Treatment of leber congenital amaurosis due to RPE65 mutations by ocular subretinal injection of adeno-associated virus gene vector: short-term results of a phase I trial. Hum Gene Ther 2008;19:979–90.
17. Maguire AM, Simonelli F, Pierce EA, et al. Safety and efficacy of gene transfer for Leber's congenital amaurosis. N Engl J Med 2008;358:2240–8.
18. Bainbridge JWB, Smith AJ, Barker SS, et al. Effect of gene therapy on visual function in Leber's congenital amaurosis. N Engl J Med 2008;358:2231–9.
19. Georgiadis A, Duran Y, Ribeiro J, et al. Development of an optimized AAV2/5 gene therapy vector for Leber congenital amaurosis owing to defects in RPE65. Gene Ther 2016;23:857–62.
20. Banin E, Obolensky A, Hemo Y, et al. Phase I gene therapy trial in Israeli patients with leber congenital amaurosis caused by a founder RPE65 mutation: safety and efficacy update with up to two years of follow-up. Invest Ophthalmol Vis Sci 2013;54:2709.
21. Le Meur G, Stieger K, Smith AJ, et al. Restoration of vision in RPE65-deficient Briard dogs using an AAV serotype 4 vector that specifically targets the retinal pigmented epithelium. Gene Ther 2007;14:292–303.
22. Bainbridge JWB, Mehat MS, Sundaram V, et al. Long-term effect of gene therapy on Leber's congenital amaurosis. N Engl J Med 2015;372:1887–97.
23. Jacobson SG, Cideciyan AV, Roman AJ, et al. Improvement and decline in vision with gene therapy in childhood blindness. N Engl J Med 2015;372:1920–6.
24. Ashtari M, Cyckowski LL, Monroe JF, et al. The human visual cortex responds to gene therapy-mediated recovery of retinal function. J Clin Invest 2011;121:2160–8.
25. Maguire AM, High KA, Auricchio A, et al. Age-dependent effects of RPE65 gene therapy for Leber's congenital amaurosis: a phase 1 dose-escalation trial. Lancet 2009;374:1597–605.
26. Jacobson SG, Cideciyan AV, Ratnakaram R, et al. Gene therapy for leber congenital amaurosis caused by RPE65 mutations: safety and efficacy in 15 children and adults followed up to 3 years. Arch Ophthalmol 2012;130:9–24.
27. Samardzija M, von Lintig J, Tanimoto N, et al. R91W mutation in Rpe65 leads to milder early-onset retinal dystrophy due to the generation of low levels of 11-cis-retinal. Hum Mol Genet 2008;17:281–92.
28. Acland GM, Aguirre GD, Bennett J, et al. Long-term restoration of rod and cone vision by single dose rAAV-mediated gene transfer to the retina in a canine model of childhood blindness. Mol Ther 2005;12:1072–82.
29. Annear MJ, Mowat FM, Bartoe JT, et al. Successful gene therapy in older Rpe65-deficient dogs following subretinal injection of an adeno-associated vector expressing RPE65. Hum Gene Ther 2013;24:883–93.
30. Bemelmans A-P, Kostic C, Crippa SV, et al. Lentiviral gene transfer of RPE65 rescues survival and function of cones in a mouse model of Leber congenital amaurosis. PLoS Med 2006;3:e347.
31. Kostic C, Crippa SV, Pignat V, et al. Gene therapy regenerates protein expression in cone photoreceptors in Rpe65(R91W/R91W) mice. PLoS One 2011;6:e16588.
32. Bennicelli J, Wright JF, Komaromy A, et al. Reversal of blindness in animal models of leber congenital amaurosis using optimized AAV2-mediated gene transfer. Mol Ther 2008;16:458–65.
33. Annear MJ, Bartoe JT, Barker SE, et al. Gene therapy in the second eye of RPE65-deficient dogs improves retinal function. Gene Ther 2011;18:53–61.
34. Narfström K, Vaegan, Katz M, Bragadottir R, Rakoczy EP, Seeliger M. Assessment of structure and function over a 3-year period after gene transfer in RPE65-/- dogs. Doc Ophthalmol 2005;111:39–48.
35. Bemelmans A-P, Kostic C, Cachafeiro M, et al. Lentiviral gene transfer-mediated cone vision restoration in RPE65 knockout mice. Adv Exp Med Biol 2008;613:89–95.
36. Schambach A, Bohne J, Baum C, et al. Woodchuck hepatitis virus post-transcriptional regulatory element deleted from X protein and promoter sequences enhances retroviral vector titer and expression. Gene Ther 2006;13:641–5.
37. Dinculescu A, Glushakova L, Min S-H, Hauswirth WW. Adeno-associated virus-vectored gene therapy for retinal disease. Hum Gene Ther 2005;16:649–63.
38. Ehnes A, Wenner Y, Friedburg C, et al. Optical coherence tomography (OCT) device independent intraretinal layer segmentation. Transl Vis Sci Technol 2014;3:1.
39. Rosolen SG, Rigaudière F, Le Gargasson J-F, Brigell MG. Recommendations for a toxicological screening ERG procedure in laboratory animals. Doc Ophthalmol 2005;110:57–66.
40. Rosolen SG, Kolomiets B, Varela O, Picaud S. Retinal electrophysiology for toxicology studies: applications and limits of ERG in animals and ex vivo recordings. Exp Toxicol Pathol 2008;60:17–32.
41. Lachapelle P, Rufiange M, Dembinska O. A physiological basis for definition of the ISCEV ERG standard flash (SF) based on the photopic hill. Doc Ophthalmol 2001;102:157–62.
42. Rufiange M, Dassa J, Dembinska O, et al. The photopic ERG luminance-response function (photopic hill): method of analysis and clinical application. Vision Res 2003;43:1405–12.
43. Amado D, Mingozzi F, Hui D, et al. Safety and efficacy of subretinal readministration of a viral vector in large animals to treat congenital blindness. Sci Transl Med 2010;2:21ra16.
44. Binley K, Widdowson P, Loader J, et al. Transduction of photoreceptors with equine infectious anemia virus lentiviral vectors: safety and biodistribution of StarGen for Stargardt disease. Invest Ophthalmol Vis Sci 2013;54:4061–71.
45. Binley K, Widdowson PS, Kelleher M, et al. Safety and biodistribution of an equine infectious anemia virus-based gene

therapy, RetinoStat(®), for age-related macular degeneration. Hum Gene Ther 2012;23:980–91.
46. Zallocchi M, Binley K, Lad Y, et al. EIAV-based retinal gene therapy in the shaker1 mouse model for usher syndrome type 1B: development of UshStat. PLoS One 2014;9:e94272.
47. Ikeda Y, Yonemitsu Y, Miyazaki M, et al. Acute toxicity study of a simian immunodeficiency virus-based lentiviral vector for retinal gene transfer in nonhuman primates. Hum Gene Ther 2009;20:943–54.
48. Thomas JA, Gagliardi TD, Alvord WG, Lubomirski M, Bosche WJ, Gorelick RJ. Human immunodeficiency virus type 1 nucleocapsid zinc-finger mutations cause defects in reverse transcription and integration. Virology 2006;353:41–51.
49. Luna G, Kjellstrom S, Verardo MR, et al. The effects of transient retinal detachment on cavity size and glial and neural remodeling in a mouse model of X-linked retinoschisis. Invest Ophthalmol Vis Sci 2009;50:3977–84.
50. Sakai T, Calderone JB, Lewis GP, Linberg KA, Fisher SK, Jacobs GH. Cone photoreceptor recovery after experimental detachment and reattachment: an immunocytochemical, morphological, and electrophysiological study. Invest Ophthalmol Vis Sci 2003;44:416–25.
51. Testa F, Maguire AM, Rossi S, et al. Three-year follow-up after unilateral subretinal delivery of adeno-associated virus in patients with Leber congenital amaurosis type 2. Ophthalmology 2013;120:1283–91.
52. Fischer MD, Hickey DG, Singh MS, MacLaren RE. Evaluation of an optimized injection system for retinal gene therapy in human patients. Hum Gene Ther Methods 2016;27:150–8.
53. Verardo MR, Lewis GP, Takeda M, et al. Abnormal reactivity of muller cells after retinal detachment in mice deficient in GFAP and vimentin. Invest Ophthalmol Vis Sci 2008;49:3659–65.
54. Lewis GP, Chapin EA, Luna G, Linberg KA, Fisher SK. The fate of Müller's glia following experimental retinal detachment: nuclear migration, cell division, and subretinal glial scar formation. Mol Vis 2010;16:1361–72.
55. Lewis GP, Sethi CS, Carter KM, Charteris DG, Fisher SK. Microglial cell activation following retinal detachment: a comparison between species. Mol Vis 2005;11:491–500.
56. Guérin CJ, Lewis GP, Fisher SK, Anderson DH. Recovery of photoreceptor outer segment length and analysis of membrane assembly rates in regenerating primate photoreceptor outer segments. Invest Ophthalmol Vis Sci 1993;34:175–83.
57. Sweigard JH, Matsumoto H, Smith KE, et al. Inhibition of the alternative complement pathway preserves photoreceptors after retinal injury. Sci Transl Med 2015;7:297ra116.
58. Wang J, Zarbin M, Sugino I, Whitehead I, Townes-Anderson E. RhoA signaling and synaptic damage occur within hours in a live pig model of CNS injury, retinal detachment. Invest Ophthalmol Vis Sci 2016;57:3892–906.
59. Guérin CJ, Anderson DH, Fisher SK. Changes in intermediate filament immunolabeling occur in response to retinal detachment and reattachment in primates. Invest Ophthalmol Vis Sci 1990;31:1474–82.
60. Narala R, Scarinci F, Shaarawy A, Simonett JM, Flaxel CJ, Fawzi AA. Longitudinal quantitative evaluation of photoreceptor volume following repair of macula-off retinal detachment. Retina 2016;36:1432–8.
61. Anand V, Chirmule N, Fersh M, Maguire AM, Bennett J. Additional transduction events after subretinal readministration of recombinant adeno-associated virus. Hum Gene Ther 2000;11:449–57.
62. Cideciyan AV, Jacobson SG, Beltran WA, et al. Human retinal gene therapy for Leber congenital amaurosis shows advancing retinal degeneration despite enduring visual improvement. Proc Natl Acad Sci U S A 2013;110:E517–25.
63. Kostic C, Chiodini F, Salmon P, et al. Activity analysis of housekeeping promoters using self-inactivating lentiviral vector delivery into the mouse retina. Gene Ther 2003;10:818–21.
64. Yáñez-Muñoz RJ, Balaggan KS, MacNeil A, et al. Effective gene therapy with nonintegrating lentiviral vectors. Nat Med 2006;12:348–53.

APPENDIX

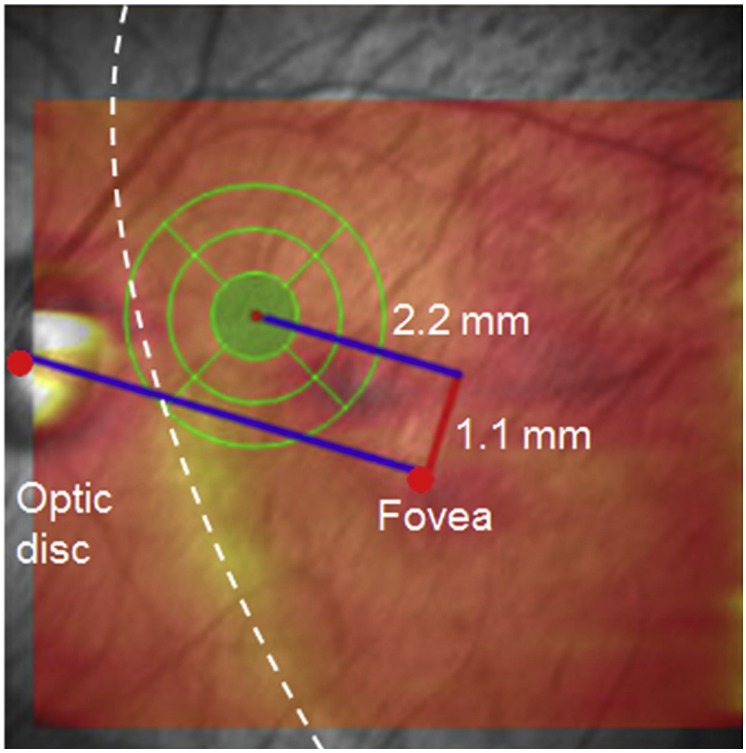

Supplementary Fig 1. Localization of the region of interest for segmentation of retinal layers over an identical area within the detached retina in all injected eyes, using a custom algorithm. Heat map of the total retinal thickness superimposed over the infrared reflectance image of the left eye of animal 1A, at day 30 after injection. The green disc at the center of the circular grid represents the 1-mm diameter region of interest, located 1.1 mm superior and 2.2 mm nasal to the fovea with the axis between optic disc center and fovea used as horizontal reference. A custom algorithm on the DiOCTA software was used to segment the retinal layers of this disc.

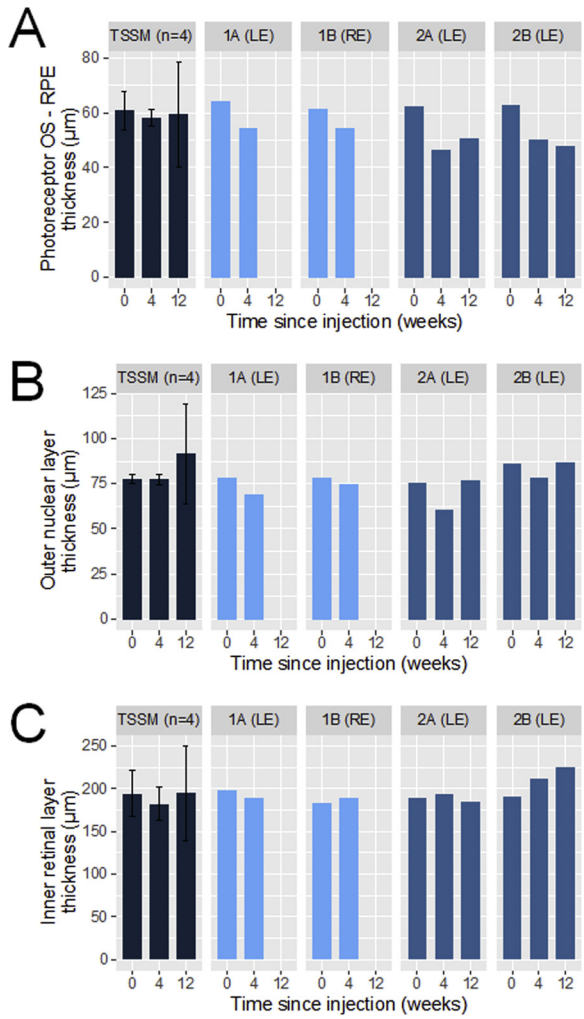

Supplementary Fig 2. Segmentation of retinal layers at the level of a 1-mm diameter circular region of interest localized within the detached area of all subretinally injected eyes. The region of interest is described in Supplementary Fig 1. (**A**) The thickness of the photoreceptor outer segments/retinal pigment epithelium showed a moderate decrease in TSSM-injected eyes and a more pronounced decrease in LV-RPE65–injected eyes. In one eye (2A [LE]), there was a late re-increase of outer segment thickness. (**B**) The thickness of the outer nuclear layer was stable in TSSM-injected eyes, with an increase in variation at the 12-week time point and showed a moderate decrease in all LV-RPE65–injected eyes, followed by a late return to baseline thickness in eyes followed up until 12-weeks. (**C**) The thickness of inner retinal layers from the inner limiting membrane to the outer limit of the outer plexiform layer was globally stable after injection of TSSM, LV-RPE65 dose 1, or dose 2. OS, outer segment; RPE, retinal pigment epithelium; RE, right eye; LE, left eye.

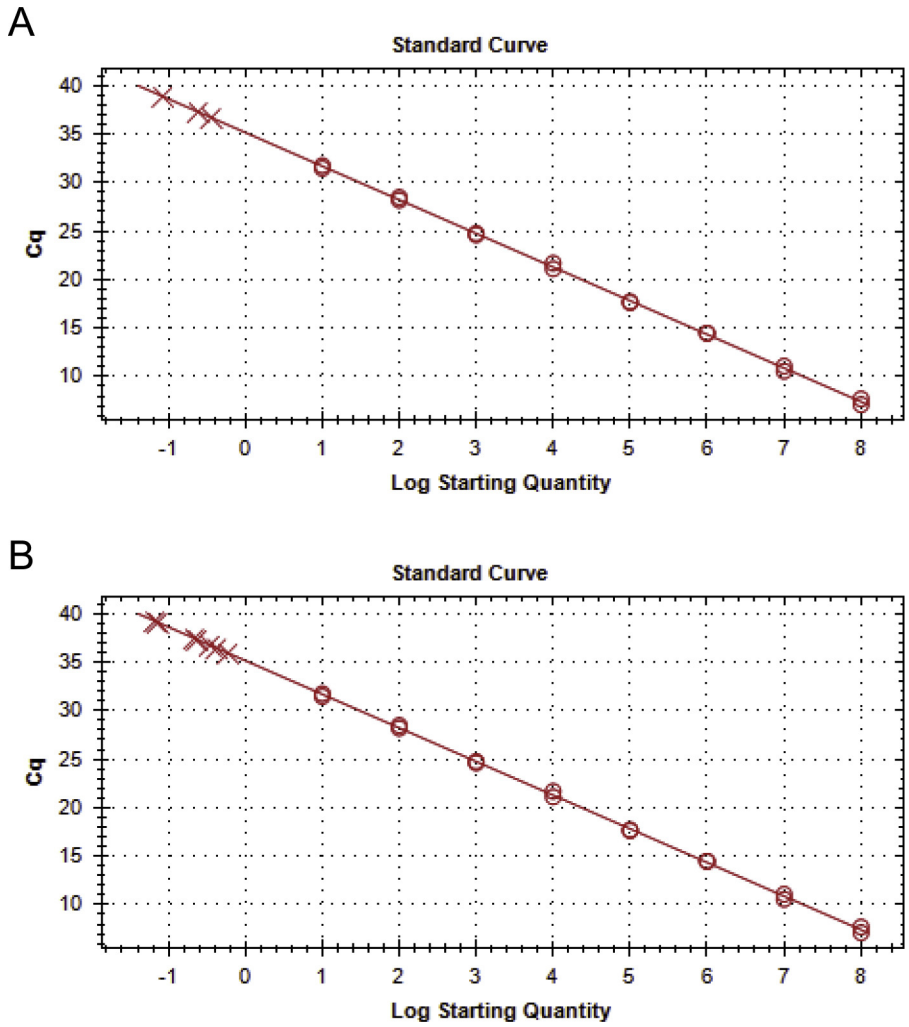

Supplementary Fig 3. Quantitative PCR standard curve and serum samples from macaque 2A. (**A**) Standard curve was established with the shuttle plasmid containing the RPE65 recombinant lentiviral genome. Open circles represent 10-fold serial dilutions of plasmid DNA ranging from 10^8 to 10 copies (duplicates). Crosses represent the negative control without DNA showing the absence of amplification (triplicate). Linear regression: r2 = 0.999. (**B**) The same standard curve as in A (open circles, duplicates) and serum samples of macaque 2A (each cross represents one sample in duplicate, n = 6 postinjection samples + 1 baseline sample) were processed in the same experiment. For all the samples tested (n = 91), either amplification did not reach the detection threshold or the Cq value did not fall below 35.

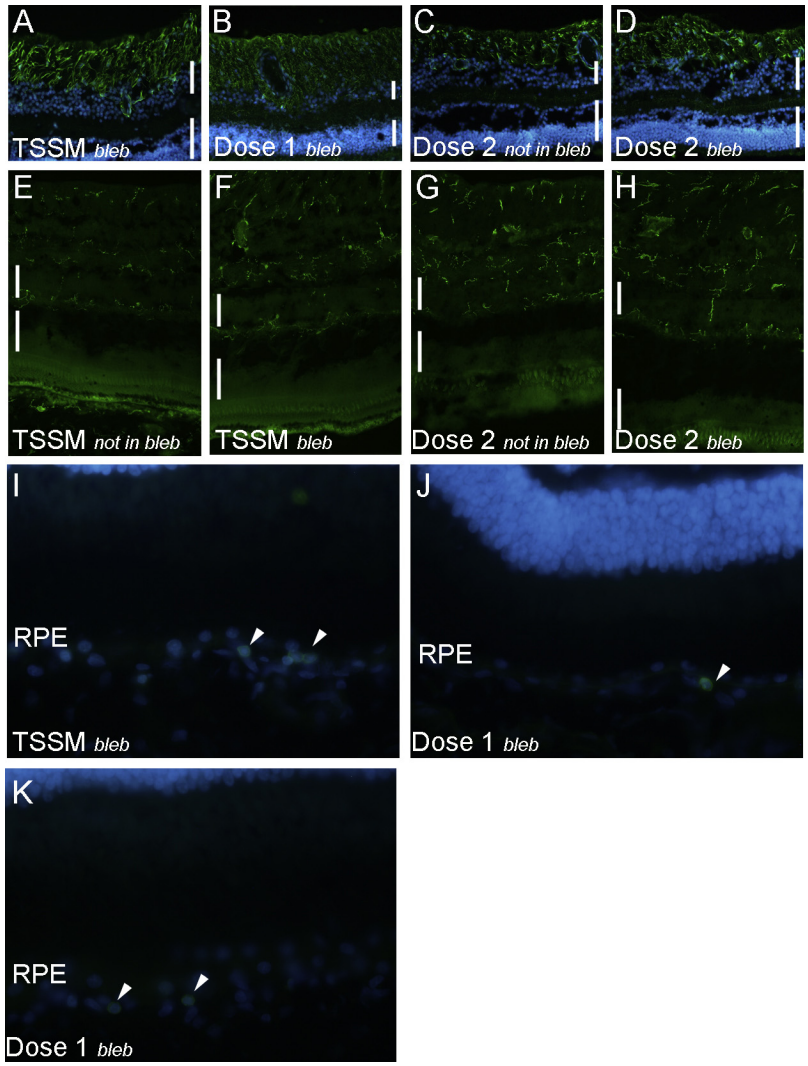

Supplementary Fig 4. Long-term evaluation of retinal reattachment using immunohistochemistry. (**A**–**D**) GFAP labeling (green) of the region of retinal detachment (detached) after injection of TSSM (**A,** animal C-RE), LV-RPE65 dose 1 (**B,** animal 1A-LE), or LV-RPE65 dose 2 (**D,** animal 2B-LE) is not different from labeling of retinal region not targeted by injection (undetached; **C,** animal 2B-LE). (**E**–**H**) Iba-1 labeling (green) of microglial cells is also similar between detached retina after injection of TSSM (**F,** animal C-RE) or after injection of LV-RPE65 dose 2 (**H,** animal 2A-LE) and undetached region of the same eye (respectively, **E** and **G**). (**I**–**K**) CD45 labeling (green) of leukocytes (arrowheads) revealed few leukocytes localized close to the RPE layer in both TSSM (**I,** animal 1A-RE) or LV-RPE65–injected eyes (**J,** animal 1B-RE, **K,** 1A-LE). **A**–**D**, **I** –**K**: DAPI counterstaining in blue; **A**–**H**: upper vertical white bars localize the inner nuclear layer and lower vertical white bars localize the outer nuclear layer; RPE, retinal pigment epithelium; GFAP, glial fibrillary acid protein.